Hydration Shell Exchange Dynamics during Ion Transfer Across the Liquid/Liquid Interface

Ilya Chorny[†] and Ilan Benjamin*

Department of Chemistry, University of California, Santa Cruz, California 95064

Received: April 8, 2005; In Final Form: June 16, 2005

We examine using molecular dynamics simulations the rate and mechanism of water molecules exchange around the Li^+ and Na^+ ions during ion transfer across the interface between water and nitrobenzene. As the ions are transferred from the water to the organic phase, they keep their first hydration shell and an incomplete second shell. The rate of water exchange between the first shell and the rest of the interfacial water molecule decreases during the transfer, which is consistent with an increase in the barrier along the ion−water potential of mean force. While in bulk water the exchange of water molecules around the Li^+ follows an associative (A) or associative interchange (I_a) type mechanism, the fraction of exchange events of type A increases at the interface. In contrast, while in bulk water the exchange of water molecules around the six coordinated Na^+ hydrated species mainly follows a dissociative mechanism, the situation at the interface involves an equilibrium interchange between the four- and five-coordinated hydrated ion. Simulation of the reversed process, in which the hydrated Li^+ ion is transferred to the aqueous phase, shows the same general behavior as a function of location from the interface.

1. Introduction

Ion transfer across the interface between two immiscible liquids is a fundamental process of importance to many fields of science and technology such as electrochemistry,[1] phase transfer catalysis,[2] and biophysics.[3] Numerous experimental and theoretical studies, which have been extensively reviewed[4−6] and are still being carried out,[7−14] have enhanced our knowledge about this process. We know more about the *structure* of the neat interface,[15−21] the electric double layer,[22−24] and the solvated ion[6,8,25−27] as the ion crosses the interface. However, despite the progress that has been made, we are still lacking a fundamental understanding of the mechanism of ion transfer and thus the ability to predict ion transfer rate constants.

One issue that has received almost no theoretical or experimental study is the rate and mechanism of solvent molecule exchange around the solvated ion during ion transfer. Knowledge about the rate of solvent exchange and its detailed mechanism is likely to contribute significantly to our understanding of the mechanism of ion transfer between two liquids. For example, it is well-known that the mobility of ions in bulk water is closely related to the residence time of water molecules within the ion's first hydration shell.[28−31] Thus, one would expect that the rate with which an ion will cross from water to an organic phase will be strongly influenced by the ability of the ion to retain its first hydration shell and by the rate with which solvent molecules are able to enter and leave the first solvation shell.

The importance of understanding the hydration shell exchange dynamics and mechanism in bulk water is clearly documented in the numerous studies of this subject.[28,30,32−39] Most of these studies have been limited to computer simulations due to experimental difficulties (such as distinguishing the response from hydration shell vs bulk molecules on the appropriate time scale). However, in recent years some experimental information is beginning to emerge. For example, the average residence time of a water molecule in the first hydration shell of ions has been determined by quasielastic neutron scattering.[40] Femtosecond mid-infrared nonlinear spectroscopy allows a determination of the spectral response of hydration shell water molecules,[41] and thus provides insight into the dynamics of first shell water molecules. These techniques can in principle be applied to ions at interfaces.[16,17,42,43] Other approaches, such as ^{7}Li NMR, can also help in this regard.[44]

Closely related to the subject of the present paper are recent molecular dynamics simulation studies of the water exchange rate around Na^+ and Li^+ in bulk water.[36,37,39,45] The rate was determined by direct simulation and the reactive flux correlation function method,[39,45] and was found to be 8.9 ± 1.3 ns^{-1} for Li^+ and 29 ± 7 ns^{-1} for Na^+, corresponding to decay times of 112 ± 16 and 34 ± 8 ps, respectively (reactive flux method). The exchange mechanism around Li^+ was discussed in detail in terms of the Langford/Gray/Merbach scheme.[46,47] According to this scheme, the exchange mechanism is classified according to the coordination number of an intermediate ion−water complex. The mechanism is called associative (A) or dissociative (D) if the exchange involves an intermediate of a higher or lower coordination number, respectively, while it is defined as interchange (I) if no such intermediate can be found. Interchange type mechanisms are further classified into an associative interchange (I_a) or a dissociative interchange (I_d) if they resemble associative or dissociative mechanisms, respectively. Most of the exchanges found around Li^+ were of types A (45%) and I_a (40%), with no type D observed.[39] While no detailed statistics were reported for Na^+, there was a significant number of the type D mechanism (from the most probable hydration number of six).[45]

* Address correspondence to this author. E-mail: benjamin@chemistry.ucsc.edu.

[†] Present address: Department of Pharmaceutical Chemistry, University of California, San Francisco, CA.

10.1021/jp051836x CCC: $30.25
Published on Web 08/06/2005

The purpose of this paper is to determine to what extent the unique boundary between two immiscible liquids manifests itself in the rate and mechanism with which water molecules are exchanged between the coordination shell and the surrounding interfacial water molecules. Previous theoretical work by us[25,48,49] and others[8,9,13,26] has demonstrated that during the transfer of small ions from the aqueous to the organic phase, a significant retention of water molecules in the ion's coordination shell is possible, which results in a significant perturbation of the neat interface. Even the transfer of large ions involves the formation of water "fingers". In addition to affecting the rate of ion transfer, this was shown to have important implications for solvation dynamics,[50,51] chemical reactions,[52,53] and vibrational relaxation.[54,55] However, no discussions of the actual dynamics of the water exchange was attempted. While the focus here is a comparison with the exchange process occurring in bulk water, recent experimental developments[12,44] suggest that the insight gained will be useful in interpreting both ion transfer data and solvent relaxation dynamics at liquid/liquid interfaces.

It is important to stress that the computer simulations of ion transfer across the interface between two immiscible liquids that have been published and those that are described here do not exactly correspond to the classic experimental situation in an electrochemical cell (where a steady-state current with supporting electrolyte solution is established and monitored). However, these simulations attempt to obtain insight into the molecular level structure and dynamics that underline the actual ion transfer process. This insight is valuable for the development of simple analytical theories and for a qualitative understanding of the mechanism by which an ion is transferred between two phases.

This paper is organized as follows: In section 2, we briefly describe the systems, the potential energy used, and the methodology of computing the potential of mean force for water exchange and the exchange dynamics. In section 3, we describe the results of a set of calculations where the ion is placed at different locations with respect to the interface. In section 4, we examine for the case of a Li^+ ion the relevance of these calculations to the actual nonequilibrium transfer of the ion back to the aqueous phase. Conclusions are given in section 5.

2. Systems and Methods

The molecular system studied includes 986 water molecules, 252 nitrobenzene molecules, and either a Na^+ or a Li^+ ion. The molecules are placed in a "box" with dimensions $L_x \times L_y \times L_z$ ($L_x = L_y = 31.3$ Å, $L_z > L_x$). Periodic boundary conditions in the three dimensions give rise to two liquid interfaces at $Z = 0$, $\pm L_z$. The reaction field method ($\epsilon = 20$) is used to calculate the contribution of the long-range forces outside the switching distance of $r = L_x/2$.

The water is modeled using a flexible SPC potential, which has been shown to describe reasonably well the interfacial properties of water.[6] The nitrobenzene is described using a flexible, all-atom model with an intramolecular potential based on harmonic bond stretching and bending, a cosine series for the torsion and improper torsion terms. The intermolecular interactions are modeled using the standard Lennard-Jones plus electrostatic terms. All the intramolecular and intermolecular potential parameters have been given in a previous publication.[56] The Bertholet (arithmetic) rule for mixtures[57] is used to determine the water−nitrobenzene liquid Lennard-Jones parameters. This model has been shown to give reasonable properties of the interface, including the surface tension[56] and interface width.[58]

The ion−water and ion−nitrobenzene interaction potentials are also modeled using a Lennard-Jones plus electrostatic term with parameters determined using the mixing rule for mixtures and the Lennard-Jones ionic parameters: $\epsilon_{Na^+} = 0.1153$ kcal/mol, $\sigma_{Na^+} = 2.275$ Å, $\epsilon_{Li^+} = 0.1333$ kcal/mol, and $\sigma_{Li^+} = 1.594$ Å (and, of course, a charge of +1 au on each ion). While more accurate many-body water−ion potentials have been developed,[59,60] we opted for this simple model to be consistent with the nitrobenzene−ion (about which very little is known) description. These parameters give an acceptable description of the structure, the hydration free energy (-93 ± 2 kcal/mol for Na^+ and -109 ± 2 kcal/mol for Li^+, compared with the experimental values of −89 and −114 kcal/mol, respectively), and the free energy of transfer from water to nitrobenzene (6.1 ± 0.7 kcal/mol for Na^+ and 7.3 ± 0.6 kcal/mol for Li^+, compared with the experimental values of 8 and 9 kcal/mol, respectively), in reasonable agreement with other simulations[28,29,39] and with experimental data.[61]

Several types of simulations are carried out for each ion in bulk water and at different locations across the water/nitrobenzene interface.

(a) Long (2 ns) equilibrium simulations in bulk water and in each of 11 different locations at the liquid/liquid interface are used to compute radial distribution functions, solvation shell structure, and water molecule exchange events with the hydration shell of each ion.

Since the ions prefer the aqueous phase to the organic phase, window potentials U_{win} are used to increase the number of configurations at each interface location. This potential prevents the ion from drifting out of a $w = 3$ Å wide slab, but it is zero when the ion is inside the slab:

$$U_{win}(z_{ion}) = kH(\zeta)\zeta^3; \qquad \zeta = |z_{ion} - c| - w/2 \qquad (1)$$

where c is the center of the slab and $H(\zeta)$ is the unit step function ($H(\zeta) = 0$ for $\zeta \leq 0$ and $H(\zeta) = 1$ for $\zeta > 0$). The different configurations are obtained from the normal fluctuations in ion positions in neighboring overlapping windows. (For example, during the 2 ns trajectory with the ion constraint to be in the interval [5 Å, 8 Å], a configuration with the ion near $Z = 8$ Å is used as the initial configuration for the simulation in the [7 Å, 10 Å] window, etc.)

The Radial distribution functions are used to compute the orientationally averaged potential of mean force (PMF) along the water−ion distance r:

$$W(r) = -\beta^{-1} \ln[g(r)] \qquad (2)$$

(b) Because the accuracy of $g(r)$ in the region between the first and second hydration shell is poor, the PMF in this region is improved using the average force integration method. This is done by constraining one of the water−ion distances r to 10 different values in the vicinity of the transition state and by using a 200 ps trajectory to calculate the average force along r. This average force is integrated with the integration constant chosen so that the resulting PMF matches the $W(r)$ calculated from the $g(r)$, as was done in ref 39.

(c) The 2 ns simulations are used to generate independent configurations where one of the water molecules is constrained to be at the transition state. These configurations are used to run reactive flux correlation function calculations in the bulk and at two of the interface regions, to determine the correction to the transition state theory rate constant.

(d) Additional calculations are performed to check to what degree the water exchange dynamics and the flux correlation function results are affected by the window potential (used in the calculations above to increase the statistical accuracy). This

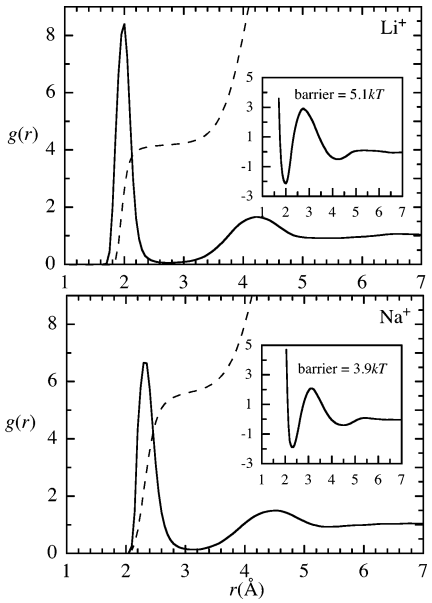

Figure 1. Oxygen−ion radial distribution function (solid lines), the running hydration numbers (dashed lines), and the potential of mean force (inserts) in units of kT with $T = 298$K for Li^+ (top panel) and Na^+ (bottom panel) in bulk water.

is done by starting from a hydrated Li^+ ion in the organic phase, removing the window potential, and letting the ion diffuse toward the aqueous phase. Twenty different trajectories, each 0.5 ns long starting from $Z = 22$ Å, are used. Water exchange events are monitored during the transfer of the ion back to the aqueous phase. Configurations where the ion Z position is at a selected interval are used to compute the flux correlation function, as explained above.

All the above simulations are carried out at a fixed temperature of $T = 298$ K, using periodic velocity rescaling. The integration of the equations of motion is performed using the velocity version of the Verlet algorithm,[62] with a time step of 0.5 fs.

3. Results and Discussion

3.1. Hydration Shell Structure. In Figure 1, we show the radial distribution function and the potential of mean force for the Li^+ and Na^+ ions in bulk water. The results are in reasonable agreement with previously published calculations and experiments.[63] Each radial distribution function clearly depicts the range of the ion−water distances (measured from the ion to the oxygen atom) that correspond to the first coordination shell. If this is taken to be the location of the first minimum in $g(r)$, we find $r_{min}(Li^+) = 2.76 \pm 0.03$ Å and $r_{min}(Na^+) = 3.10 \pm 0.03$ Å. The dashed line in each panel gives the running coordination number:

$$n(r) = \int_0^r 4\pi\rho r^2 g(r)\, dr,$$

where $\rho = 0.0334$ Å^{-3} is the bulk density of water at the temperature of the simulation. If one defines the first coordination number as $n(r_{min})$, one obtains 4.07 ± 0.03 for Li^+ and 5.72 ± 0.07 for Na^+. These values are in agreement with most calculations[39] and experimental data.[63]

The potential of mean force for the ion−water (not corrected for the centrifugal contribution of $kT \ln r^2$) is shown in the insert of each panel. The indicated barrier is also in good agreement with previous calculations (it should be decreased by $\sim 0.6kT$ if the centrifugal correction is included). With this barrier,

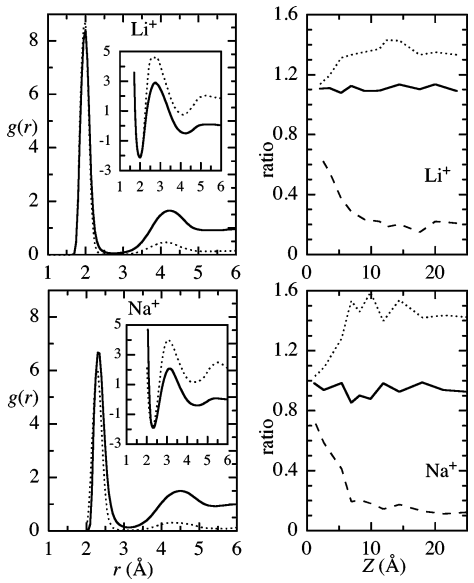

Figure 2. The left panels compare the radial distribution function, the running hydration number, and the potential of mean force of Figure 1 (bulk water) with the data from one of the interfacial systems as explained in the text. The right panels show the height of the first peak of $g(r)$ (solid lines), the height of the second peak of $g(r)$ (dashed lines), and the barrier height (dotted lines) relative to bulk water, for all the interfacial systems, as a function of the ion location Z.

transition state theory gives for the rate constant of the exchange "reaction"

$$k_{TST} = (2\pi\beta\mu)^{-1/2} \frac{(r^*)^2 e^{-\beta W(r^*)}}{\int_0^{r^*} r^2 e^{-\beta W(r^*)}\, dr} \qquad (3)$$

where μ is the water−ion reduced mass and r^* is the location of the barrier (which is very close to r_{min}). This formula and the data in Figure 1 give for the mean residence time of a water molecule in the first hydration shell ($\tau \approx k_{TST}^{-1}$) the values 16 ps for Li^+ and 6 ps for Na^+. As we will see below, the actual times are longer by a factor of approximately 5 because of deviations from the transition state theory due to barrier recrossings.[39,45]

Figure 2 presents the orientationally averaged $g(r)$ and the potential of mean force $W(r)$ when each ion is gradually moved from the Gibbs dividing surface ($Z = 0$, the plane where the average density of water is 50% of the bulk value) to the bulk of the organic phase. The left panels show as an example a comparison of the results in bulk water (solid line) to the results at a window spanning the region 7 Å $< Z <$ 10 Å. The right panels summarize the results in all 11 windows. Specifically shown are the height of the first peak of $g(r)$ relative to bulk water (solid line), the height of the second peak of $g(r)$ relative to bulk water (dashed line), and the barrier height relative to that in bulk water (dotted line).

Several important observations can be made regarding these equilibrium structural data.

(a) The structure of the first hydration shell is almost independent of the interfacial location of the ion. The height of the first peak of the Li^+−O radial distribution function is nearly constant at about 120% of the value in bulk water. Its location is very nearly constant at around 2 Å, and it is slightly narrower. The coordination number fluctuates between 4.00 ± 0.05 and 4.06 ± 0.05 for the different windows. Similarly for Na^+, the height of the first peak of $g(r)$ remains almost constant at 90% of the value in bulk water, while a slight narrowing of the

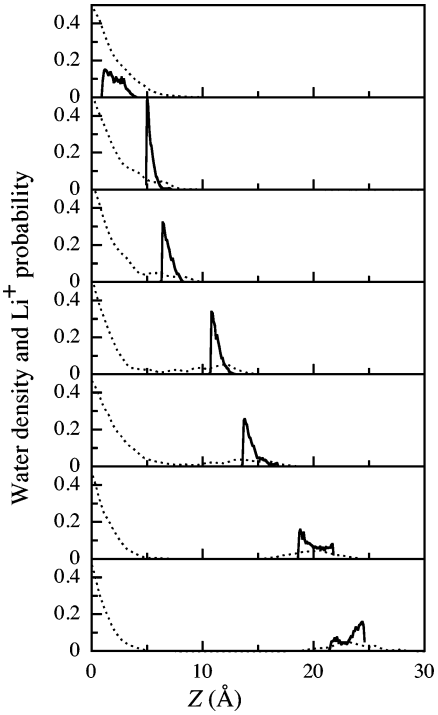

Figure 3. Dotted lines: The tail of the water density profile (measured relative to the density of bulk water). Solid lines: the Li^+ ion position probability distribution (unit area normalized). Shown for several interfacial systems, in each of which the ion is confined to a 3Å wide window. The nitrobenzene density profile is not shown for clarity.

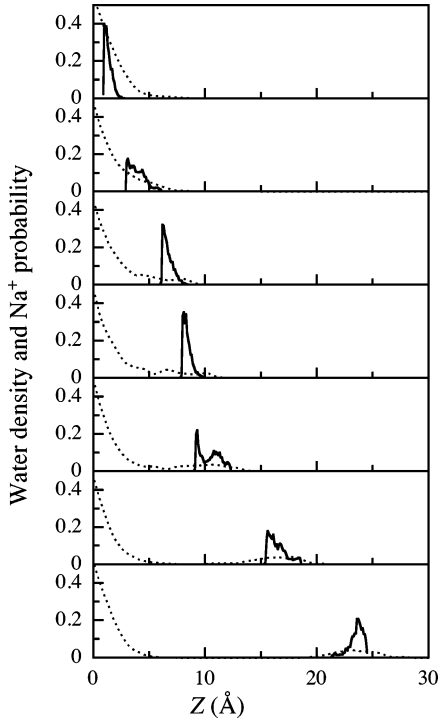

Figure 4. Same as Figure 3 for Na^+ at the water/nitrobenzene interface.

distribution and a very slight shift to a smaller first peak location are observed. The coordination number (not shown) fluctuates wildly in the range between 5.4 and 4.1, with large statistical uncertainties (between 0.2 and 0.5). We will see that this is related to the much larger "fluidity" of the first hydration shell of Na^+ compared with the tighter first hydration shell of Li^+.

(b) There is a significant and rapid drop in the height of the second peak for both ions as the ion is moved from Z = 0 to 10 Å, after which the height remains nearly constant at about 10−20% of the bulk value. We will show later that this behavior is closely related to a change in the structure of interfacial water.

(c) The barrier to escape from the first hydration shell increases to about 130% of the bulk value for Li^+ and to about 150% of the bulk value for Na^+ as the ion is moved from Z = 0 to 10 Å. The increase in barrier height reflects the larger force required to break the ion−water "bond" in the lower dielectric medium, a phenomenon well-known from other interfacial systems[52] and supercritical liquids.[64−66] This suggests a slower exchange rate at the interface and a tightening of the hydration shell as the ion is forced into the organic phase.

Some insight into the observed change in the structure of the hydration shell can be gained by considering the change in the water density profile for the different interfacial systems. This is shown in Figure 3 for Li^+ and in Figure 4 for Na^+. Each figure depicts the water density profile and the ion location probability distribution in a selection of 7 of the 11 interfacial systems. As each ion is moved from the Gibbs surface region ($Z = 0$) toward the organic phase, the water density profile shows increased water excess in the organic phase. Note that when the ion is in the region 7 Å < Z < 10 Å, the tail of the main water lamella density profile corresponds to a density that is less than the water density in the immediate vicinity of the ion. This is the region where the ion hydration shell is beginning to be well separated from the rest of the interfacial water. It is still connected to the water lamella by a water "finger", which becomes elongated as the ion is further moved to larger Z values. When the position of the Li^+ ion reaches around 15 Å (18 Å for Na^+), the hydration shell breaks away from the main water, and the "finger" retracts. A further increase in Z as the ion diffuses to the bulk of the organic phase shows that the ion keeps a water hydration shell in the organic phase. It is interesting to note that several additional water molecules accompany the hydrated ion and give rise to a loose and incomplete 2nd hydration shell (on our simulation time scale). The fact that Na^+ and Li^+ keep their hydration shell in the organic phase has been documented experimentally.[12,61] Our finding that several additional water molecules are likely to "hang around" the stable hydrated ions suggests that water exchange dynamics may be observed even for ions that are located in the bulk of the organic phase, as will be shown below. It is also important to stress that while the structures observed here correspond to a system where the ion is restricted to a narrow window (a computational requirement to increase statistical accuracy), very similar structures have been observed in more realistic simulations where the ion is transferred under the influence of external electric fields (with a magnitude similar to the one that exists in a typical cell) from the aqueous to the organic phase.[25,49]

3.2. Water Exchange Dynamics During Ion Transfer to the Organic Phase. The exchange dynamics is followed in bulk water and for each of the interfacial systems by recording the number of water molecules in the first hydration shell at 25 fs intervals and recording the oxygen−ion distance for each water molecule in the first hydration shell and for each water molecule that enters the region between the first and second peaks of $g(r)$.

The process of water molecule exchange is a random rare event, and before we proceed with a quantitative discussion of the exchange rate, some insight into the rate and mechanism can be qualitatively gained from an examination of the time-dependent hydration shell number. Figure 5 shows time segments of 500 ps for Li^+ in bulk water and in several locations at the interface, and Figure 6 shows time segments of 250 ps

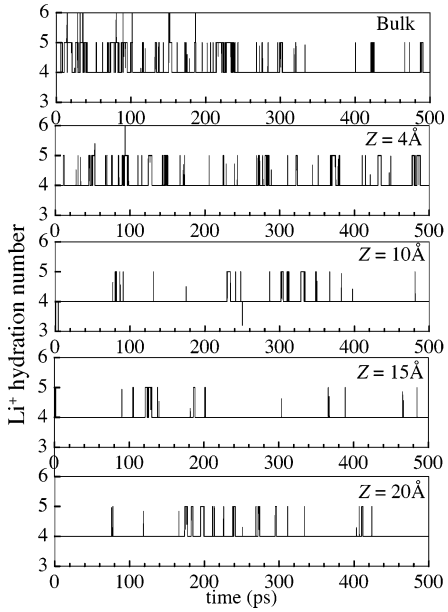

Figure 5. Time segments (0.5 ns) showing the time-dependent hydration number of Li^+ at several interfacial locations and in bulk water.

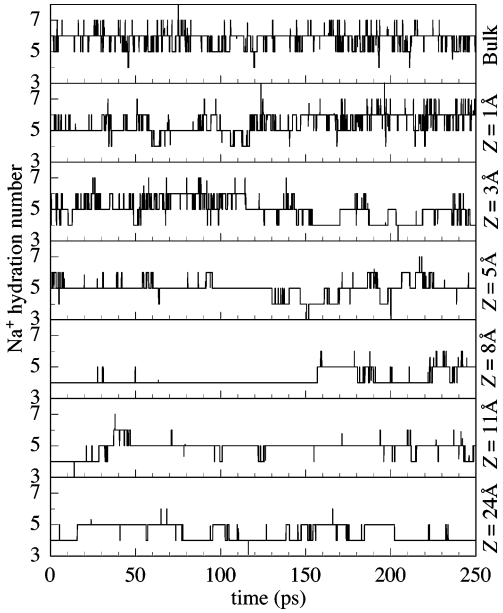

Figure 6. Time segments (0.25 ns) showing the time-dependent hydration number of Na^+ at several interfacial locations and in bulk water.

for Na^+ in bulk water and at several interface locations. Exchange events are observed as vertical jumps as a water molecule enters or leaves the first hydration shell. Only those events in which the water molecule remains in the hydration shell for more than 1 ps before leaving, or remains outside the hydration shell for more than 1 ps before entering, are used to determine an (approximate) exchange rate. Further, while Figures 5 and 6 show all exchange events, it is also possible to separate those where the identity of the water molecule that left or entered the shell has changed.

For Li^+, almost all events involve a water molecule entering the hydration shell, and either leaving immediately (within 0.1 ps) or staying for a time interval of up to 10 ps and then leaving. This is consistent with the associative (A) and associative interchange (I_a) mechanisms found by Spångberg et al in bulk water.[39] This process is only mildly reduced in frequency when the Li^+ is located 4 Å into the organic phase, but the frequency is significantly reduced when the ion is at the tip of a short water finger ($Z = 10$ Å). Further increasing Z to a value corresponding to the longest water finger ($Z = 15$ Å) only slightly reduces the frequency of the exchange events, and these exchange events are clearly observed even when the ion is separated from the water ($Z = 20$ Å). In this case, the exchange events involve water molecules moving from the partial second shell into the first shell. An exact counting of all the events further shows that the probability of the "A" type mechanism increases and that of type I_a decreases as the ion is moved to the organic phase. This can be explained by the notion that for a water molecule to leave the hydration shell in a region where there are few water molecules around, it must first find a hydrogen-bonding partner. Thus, once an $Li^+(H_2O)_5$ complex is formed at the interface (a less likely event at the interface than in the bulk), it tends to live longer, which is consistent with a type "A" mechanism.

The exchange events around Na^+ are more frequent, so we only show a 250 ps segment out of the 2 ns trajectory at each interface location. The exchange dynamics are more complex here because the most stable hydrated species changes identity as the ion moves from bulk water deeper into the organic phase. In bulk water, the most likely species is $Na^+(H_2O)_6$ (accounting for 71% of all configurations), followed by $Na^+(H_2O)_5$ (21%), and the rest are either transitional species or a few percent of the four- and seven-coordinated species. The average residence time for a water molecule in the six-coordinated species determined from the trajectories is 25 ± 10 ps. A more accurate value determined using the flux correlation function (see below) is 30 ± 3 ps. Exchange events with respect to the $Na^+(H_2O)_6$ species are mainly of the dissociative (D) or interchange dissociative (I_d) type. However, most of the exchange events for the $Na^+(H_2O)_5$ species can be categorized as associative type. These results are in qualitative agreement with the work of Rey and Hynes, who categorize the exchange events around the six-coordinated species as S_N1- and S_N2-like processes.[45] However, a detailed study by Spangberg, Wojcik, and Hermansson[36] suggests that most exchange events around the $Na^+(H_2O)_6$ species are associative. This discrepancy is probably due to the fact that the potential energy functions for the water and the water$-Na^+$ interactions used in their paper are quite different from the one used here, giving, for example, a significantly larger average coordination number of 6.5. This sensitivity of the mechanism to the choice of the potential energy functions deserves additional study.

As the Na^+ is transferred to the organic phase, initially the most likely species is $Na^+(H_2O)_5$, with a substantial fraction of $Na^+(H_2O)_4$. Further movement of the ion toward the organic phase (finally resulting from a separation from the bulk water phase) makes the fraction of the four-coordinated species larger, but there is always a significant probability of observing relatively long-lived five-coordinated species. The frequency of the exchange events is diminished, and the system behavior can be better characterized as an equilibrium $Na^+(H_2O)_4 + H_2O \leftrightarrow Na^+(H_2O)_5$, with an equilibrium constant of near unity, so the characterization scheme in terms of associative, dissociative, or interchange type mechanism loses its utility in this case.

Despite the relatively long direct simulation at each interfacial location, the rarity of the exchange events prevents us from reporting a quantitative branching ratio for the different exchange pathways. However, the qualitative observation that the average residence time at the interface is longer than in the

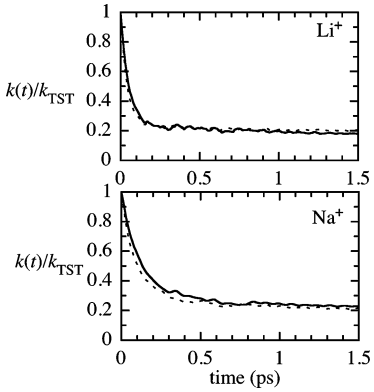

Figure 7. Normalized reactive flux correlation function for water exchange around Li^+ and Na^+ in bulk water (solid lines) and at the water/nitrobenzene interface (dotted lines).

bulk, which is consistent with the increase in the barrier height noted in section 3.1, can be made quantitative. The transition state theory rate determined from the barrier can be corrected for barrier recrossing dynamics. This can be easily and efficiently done[39,67,68] by initiating 500 independent trajectories at the top of the barrier, with random velocities selected from a flux-weighted Maxwell−Boltzmann distribution.[67] The trajectories are integrated forward and backward in time, and the reaction coordinate R is followed for 1.5 ps (in each direction). The normalized flux correlation function is[68]

$$\kappa(t) = N_+^{-1}\sum_{i=1}^{N_+}\theta[R_i^+(t) - R_{TS}] - N_-^{-1}\sum_{i=1}^{N_-}\theta[R_i^-(t) - R_{TS}] \quad (4)$$

where R_{TS} is the location of the barrier maximum, $R^{\pm}(t)$ is the value of the reaction coordinate at time t for trajectories that initially moved to the right (left), $N_{\pm}$ is the corresponding number of trajectories, and $\theta(x)$ is the unit step function.

These calculations have been carried out in the bulk and at two of the interface locations ($\langle Z\rangle = 4$ and 10 Å for Li^+ and $\langle Z\rangle = 3$ and 11 Å for Na^+) for each ion. The results given in Figure 7 show that there are extensive barrier recrossing dynamics, as is evident by the fact that the plateau value of $k(t)$ (the transmission coefficient) is significantly less than one. We get for bulk Li^+: $= 0.18 \pm 0.2$, which then gives for the decay time the value: 87 ± 7 ps and for bulk Na^+ $\kappa = 0.22 \pm 0.2$, which then gives for the decay time the value $\kappa = 30 \pm 3$ ps. The results for Na^+ are in agreement with previous calculations,[45] while the results for Li^+ are about 20% faster than previous calculations,[39] reflecting the different potential energy used and the sensitivity of the results to the exact value of the barrier height. The results for $k(t)$ in the two interface locations were almost identical with each other and to the bulk, giving in all cases a plateau value of 0.2 ± 0.2. This suggests that the barrier height data shown in Figure 2 can be directly converted to reasonably accurate decay times. These decay times are approximately twice as long at the interface as in the bulk and do not vary appreciably between the different interface locations, which is consistent with the crude values obtained from the direct dynamics calculations.

The fact that the barrier recrossing dynamics are not very sensitive to the location of the ion is consistent with the notion that the local environment around the ion is almost unchanged. The four water molecules around the Li^+ and the 5−6 around the Na^+ are hydrogen bonded to other water molecules, even if the ion is pushed deep into the organic phase. Thus, the transition

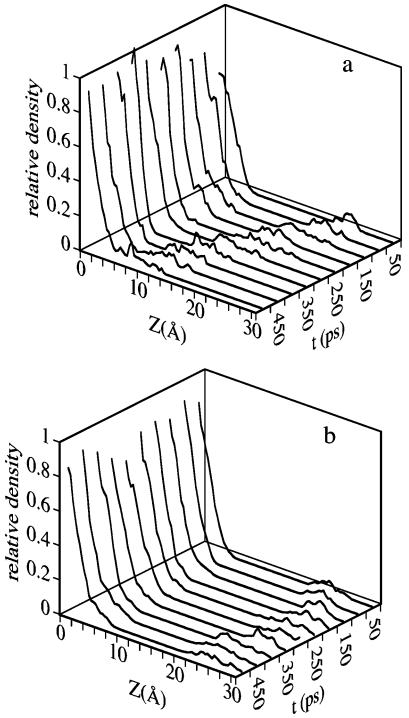

Figure 8. Time-dependent water density profiles for Li^+ ion transfer back to the aqueous phase, starting from a hydrated ion in the organic phase. In panel a, the ion gets near the Gibbs surface ($Z = 0$), while in panel b it remains in the organic phase far from the aqueous phase. The different density profiles are determined from a 10 ps average and are separated by 50 ps.

state region for a single water molecule motion relative to the hydration complex is not markedly different between the bulk and the interface. The small value of the transmission coefficient reflects the fact that the dynamics involved in water exchange are complex, so that when the high-dimensional dynamics of all the water molecules are projected onto the one-dimensional reaction coordinate, extensive recrossings are observed.

3.3. Ion Transfer Back to the Aqueous Phase. To improve statistical accuracy in the calculations described above, the ion has been constrained to be in a set of overlapping windows, each with a width of 3 Å. An important issue is to what degree the calculated structural properties and the exchange dynamics are influenced by this perturbation, and whether the dynamics without the constraints are relevant to ion transfer dynamics in realistic systems.

A hydrated ion located in the organic phase and separated from the bulk aqueous phase may diffuse back toward the aqueous phase and then spontaneously transfer across the interface. Despite the significant negative free energy of transfer, this is a slow process, and one may calculate water exchange dynamics and other properties as the ion crosses the interface. To increase statistics, we have run 20 trajectories, each 0.5 ns long, all with a hydrated Li^+ ion starting from $Z = 22$ Å (a configuration taken from one of the simulations with the ion completely detached from the water). In some of these trajectories, the ion remains in the bulk organic phase. In 9 of the trajectories, the ion reconnected to the aqueous phase while forming structures similar to the one observed in the constraint simulation: As the hydrated ion approaches the aqueous phase, hydrogen bonding between the partial second hydration shell and interfacial water molecules creates fingerlike structures. In Figure 8, we show examples of two such trajectories, where the tail of the density profiles of water in 50 ps intervals are shown for a case where the ion reaches near the Gibbs surface

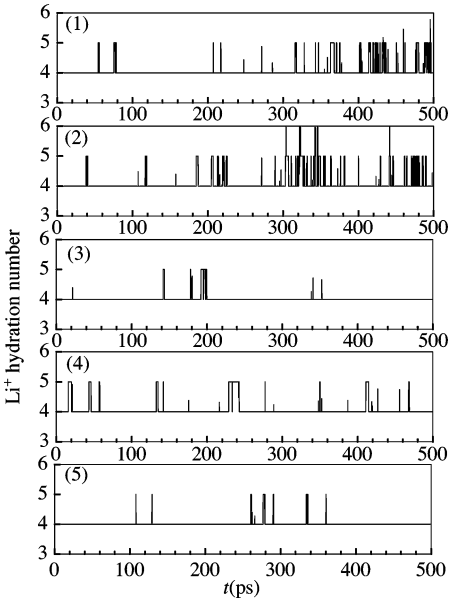

Figure 9. Time-dependent Li^+ ion hydration number in five different trajectories, each starting from the hydrated ion in the organic phase.

(panel a), and for a case where the ion remains in the organic phase on the simulation time scale (panel b). This spontaneous formation of bridges and fingerlike structures during the unconstrained transfer of ions (with and without external fields) has been previously observed.[25,48,49]

The water exchange dynamics around the ion for some of the trajectories are depicted in Figure 9. The corresponding Z position on the ion and its interaction with the two liquids are shown in Figure 10. The total interaction energy of the ion with each liquid at the interface is used to define a partial solvation coordinate: $s_{H_2O} = \{V_{ion-H_2O}(\text{interface})\}/\{V_{ion-H_2O}(\text{bulk water})\}$, with a similar expression for the nitrobenzene. While the statistics in these calculations are not sufficient to calculate accurate hydration shell lifetimes, it is obvious that as the ion gets closer to the Gibbs surface in the successful ion transfer trajectories (numbers 1 and 2), this lifetime becomes shorter, as was found in the constraint calculations. Note that the onset of increased exchange events approximately corresponds to the point where the water solvation coordinate s in Figure 10 begins to rapidly rise. In trajectories 3 and 4, the ion hydration forms a bridge with the interfacial water molecules, but the ion remains far from the interface, as is clear from examining the corresponding plots in Figure 10 (s_{H_2O} only slightly increases). In the trajectory labeled (5), the ion remains in the organic phase and does not form a bridging finger with the water phase. In all cases, our previous observation of association type exchange trajectories remains the case during the transfer.

Finally, to examine the flux correlation function, 100 configurations in which the Z_{ion} is near 4 Å and one of the hydration shell water molecules is at the transition state for an exchange event are taken from trajectory (1). These configurations are used to compute $k(t)$, as done previously. The results were essentially the same as those calculated from the constraint calculations. This is not surprising since the time scale for the decay of the flux correlation function is much shorter than the ion motion along Z. The external window potential used to constrain the ion position in the calculations described earlier does not seem to interfere with the barrier recrossing dynamics.

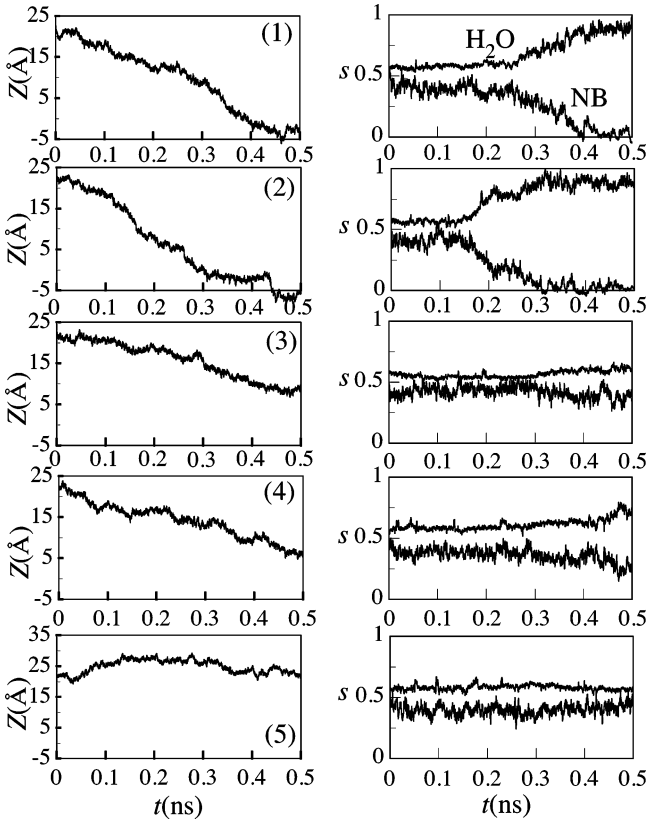

Figure 10. The position of the ion (left panels) and its normalized interaction energy with the two liquids (right panels) for the five trajectories shown in Figure 9. In each of the right panels, the top narrower line gives the water−ion interaction relative to the interaction in bulk water, and the noisier lower line gives the nitrobenznene−ion interaction relative to that of the bare ion in the organic phase.

4. Conclusions

The exchange of water molecules around a hydrated ion at the water/nitrobenzene interface has been studied for small ions that keep their hydration shell intact (Li^+) or nearly so (Na^+). A comparison with the exchange dynamics in bulk water reveals that the exchange is significantly slower, consistent with an increased barrier height to water molecules leaving or entering the hydration shell. Although slower, this exchange is observed even if the ion is in the bulk organic phase, due to rare exchange events between the first hydration shell and an (incomplete) second hydration shell. The change in the rate is accompanied by a change in the most likely path for water exchange. For Li^+, the transition to the interface increases the fraction of associative type exchanges where a water molecule first joins the hydration shell before another one, a few picoseconds later, leaves. For Na^+ in bulk water, a dominant path involves an escape of a water molecule from the six-coordinated ion before a new water molecule (immediately or a few picoseconds later) joins it. At the interface, there is an equilibrium between the four- and five-coordinated ion involving associative or dissociative type exchanges, respectively. The above conclusions for the case of Li^+ hold for the reverse case, in which the hydrated ion is allowed to transfer back to the aqueous phase.

While the above insight may be useful for the development of ion transfer rate theories, it is not clear how much of this applies to larger ions that lose part or all of their hydration shell upon transfer to the organic phase. This is left to future studies.

Acknowledgment. This work has been supported by a grant from the National Science Foundation (CHE-0345361).

References and Notes

(1) Girault, H. H.; Schiffrin, D. J. Electrochemistry of liquid−liquid interfaces. In *Electroanalytical Chemistry*; Bard, A. J., Ed.; Dekker: New York, 1989; p 1.
(2) Starks, C. M.; Liotta, C. L.; Halpern, M. *Phase Transfer Catalysis*; Chapman & Hall: New York, 1994.
(3) Arai, K.; Ohsawa, M.; Kusu, F.; Takamura, K. *Bioelectrochem. Bioenerg.* **1993**, *31*, 65.
(4) Vanysek, P. *Electrochim. Acta* **1995**, *40*, 2841.
(5) *Liquid−Liquid Interfaces*; Volkov, A. G., Deamer, D. W., Eds.; CRC Press: Boca Raton, FL, 1996.
(6) Benjamin, I. *Annu. Rev. Phys. Chem.* **1997**, *48*, 401.
(7) Marcus, R. A. *J. Chem. Phys.* **2000**, *113*, 1618.
(8) dos Santos, D. J.; Gomes, J. A. *ChemPhysChem* **2002**, *3*, 946.
(9) Kornyshev, A. A.; Kuznetsov, A. M.; Urbach, M. *J. Chem. Phys.* **2002**, *117*, 6766.
(10) Sun, P.; Zhang, Z. Q.; Gao, Z.; Shao, Y. H. *Angew. Chem., Int. Ed.* **2002**, *41*, 3445.
(11) Yatziv, Y.; Turyan, I.; Mandler, D. *J. Am. Chem. Soc.* **2002**, *124*, 5618.
(12) Osakai, T. The role of water molecules in ion transfer at the oil/water interface. In *Interfacial Catalysis*; Volkov, A. G., Ed.; Marcel Dekker: New York, 2003; p 53.
(13) Wardle, K. E.; Carlson, E.; Henderson, D.; Rowley, R. L. *J. Chem. Phys.* **2004**, *120*, 7681.
(14) Cai, C.; Tong, Y.; Mirkin, M. V. *J. Phys. Chem. B.* **2004**, *108*, 17872.
(15) Pohorille, A.; Wilson, M. A. *J. Mol. Struct.* (*THEOCHEM*) **1993**, *103*, 271.
(16) Eisenthal, K. B. *Chem. Rev.* **1996**, *96*, 1343.
(17) Richmond, G. L. *Chem. Rev.* **2002**, *102*, 2693.
(18) Mitrinovic, D. M.; Zhang, Z.; Williams, S. M.; Huang, Z.; Schlossman, M. L. *J. Phys. Chem. B* **1999**, *103*, 1779.
(19) Schlossman, M. L. *Curr. Opin. Colloid Interface Sci.* **2002**, *7*, 235.
(20) Grimm, A.; Muhlfriedel, K.; Baumann, K. H. *Chem. Ing. Tech.* **2002**, *74*, 1582.
(21) Brodard, P.; Vauthey, E. *Rev. Sci. Instrum.* **2003**, *74*, 725.
(22) Samec, Z.; Marecek, V.; Homolka, D. *J. Electroanal. Chem.* **1985**, *187*, 31.
(23) Schmickler, W. *Chem. Rev.* **1996**, *96*, 3177.
(24) Ni, H.; Amme, R. C. *J Colloid Interface Sci* **2003**, *260*, 344.
(25) Schweighofer, K. J.; Benjamin, I. *J. Phys. Chem. A* **1999**, *103*, 10274.
(26) Dang, L. X. *J. Phys. Chem. B* **1999**, *103*, 8195.
(27) Schnell, B.; Schurhammer, R.; Wipff, G. *J. Phys. Chem. B* **2004**, *108*, 2285.
(28) Impey, R. W.; Madden, P. A.; McDonald, I. R. *J. Phys. Chem.* **1983**, *87*, 5071.
(29) Ohtaki, H.; Radnai, T. *Chem. Rev.* **1993**, *93*, 1157.
(30) Lee, S. H.; Rasaiah, J. C. *J. Chem. Phys.* **1994**, *101*, 6964.
(31) Koneshan, S.; Rasaiah, J. C.; Lynden-Bell, R. M.; Lee, S. H. *J. Phys. Chem. B* **1998**, *102*, 4193.
(32) Aakesson, R.; Pettersson, L. G. M.; Sandstroem, M.; Wahlgren, U. *J. Am. Chem. Soc.* **1994**, *116*, 8705.
(33) Kowall, T.; Foglia, F.; Helm, L.; Merbach, A. E. *Chem. Eur. J.* **1996**, *2*, 285.
(34) Hartmann, M.; Clark, T.; Eldik, R. v. *J. Am. Chem. Soc.* **1997**, *119*, 7843.
(35) Rotzinger, F. P. *J. Am. Chem. Soc.* **1997**, *119*, 5230.
(36) Spångberg, D.; Wojcik, M.; Hermansson, K. *Chem. Phys. Lett.* **1997**, *276*, 114.
(37) Hermansson, K.; Wojcik, M. *J. Phys. Chem. B* **1998**, *102*, 6089.
(38) Lyubartsev, A. P.; Laasonen, K.; Laaksonen, A. *J. Chem. Phys.* **2001**, *114*, 3120.
(39) Spångberg, D.; Rey, R.; Hynes, J. T.; Hermansson, K. *J. Phys. Chem. B* **2003**, *107*, 4470.
(40) Salmon, P. S.; Howells, W. S.; Mills, R. *J. Phys. C*: *Solid State Phys.* **1987**, *20*, 5727.
(41) Kropman, M. F.; Bakker, H. J. *Science* **2001**, *291*, 2118.
(42) Benderskii, A. V.; Eisenthal, K. B. *J. Phys. Chem. A* **2002**, *106*, 7482.
(43) Steel, W. H.; Walker, R. A. *Nature* **2003**, *424*, 296.
(44) Moakes, G.; Gelbaum, L. T.; Leisen, J.; Janata, J. *Faraday Discuss. Chem. Soc.* **2005**, *129*.
(45) Rey, R.; Hynes, J. T. *J. Phys. Chem.* **1996**, *100*, 5611.
(46) Gray, H. B.; Langford, C. H. *Ligand Substitution Processes*; W. A. Benjamin: New York, 1966.
(47) Lincoln, S. F.; Merbach, A. E. *Adv. Inorg. Chem.* **1995**, *42*, 1.
(48) Benjamin, I. *Science* **1993**, *261*, 1558.
(49) Schweighofer, K. J.; Benjamin, I. *J. Phys. Chem.* **1995**, *99*, 9974.
(50) Michael, D.; Benjamin, I. *J. Chem. Phys.* **2001**, *114*, 2817.
(51) Vieceli, J.; Benjamin, I. *J. Phys. Chem. B* **2003**, *107*, 4801.
(52) Benjamin, I. *Chem. Rev.* **1996**, *96*, 1449.
(53) Winter, N.; Benjamin, I. *J. Chem. Phys.* **2005**, in press.
(54) Vieceli, J.; Chorny, I.; Benjamin, I. *J. Chem. Phys.* **2002**, *117*, 4532.
(55) Benjamin, I. *J. Chem. Phys.* **2004**, *121*, 10223.
(56) Michael, D.; Benjamin, I. *J. Electroanal. Chem.* **1998**, *450*, 335.
(57) Hansen, J.-P.; McDonald, I. R. *Theory of Simple Liquids*, 2nd ed.; Academic: London, UK, 1986.
(58) Luo, G.; Malkova, S.; Pingali, S. V.; Schultz, D. G.; Lin, B.; Meron, M.; Graber, T. J.; Gebhardt, J.; Vanysek, P.; Schlossman, M. L. *Faraday Discuss.* **2005**, *129*, 23.
(59) Dang, L. X.; Rice, J. E.; Caldwell, J.; Kollman, P. A. *J. Am. Chem. Soc.* **1991**, *113*, 2481.
(60) Spangberg, D.; Hermansson, K. *J. Chem. Phys.* **2004**, *120*, 4829.
(61) Marcus, Y. *Ion Solvation*; Wiley: New York, 1985.
(62) Allen, M. P.; Tildesley, D. J. *Computer Simulation of Liquids*; Clarendon: Oxford, UK, 1987.
(63) Cartailler, T.; Kunz, W.; Turq, P.; Bellisent-Funel, M.-C. *J. Phys. Condens. Matter* **1991**, *3*, 9511.
(64) Gao, J. L. *J. Phys. Chem.* **1994**, *98*, 6049.
(65) Westacott, R. E.; Johnston, K. P.; Rossky, P. J. *J. Phys. Chem. B* **2001**, *105*, 6611.
(66) Masia, M.; Rey, R. *J. Phys. Chem. B* **2003**, *107*, 2651.
(67) Berne, B. J.; Borkovec, M.; Straub, J. E. *J. Phys. Chem.* **1988**, *92*, 3711.
(68) Gertner, B. J.; Wilson, K. R.; Hynes, J. T. *J. Chem. Phys.* **1989**, *90*, 3537.